Suppression of inflammation and acute lung injury by the transcription factor Miz1 via repression of C/EBP-δ

Hanh Chi Do-Umehara, Cong Chen, Daniela Urich, Liang Zhou, Ju Qiu, Samuel Jang, Alia Zander, Margaret A. Baker, Martin Eilers, Peter H. S. Sporn, Karen M. Ridge, Jacob I. Sznajder, G. R. Scott Budinger, Gökhan M. Mutlu, Anning Lin & Jing Liu

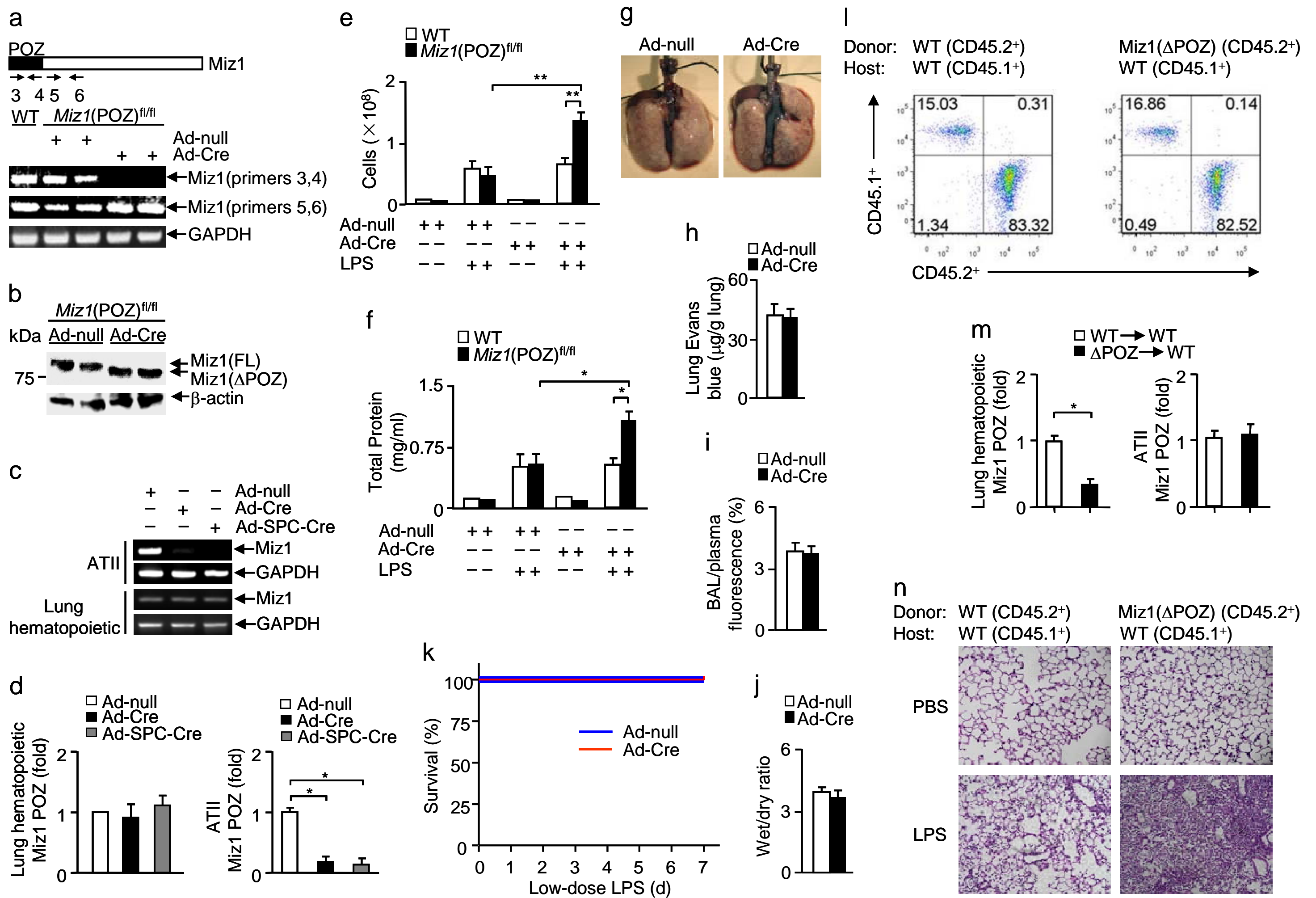

Supplementary Figure 1 Analysis of lung-specific deletion of the Miz1 POZ domain and its effects on LPS-induced inflammation in mice. (**a**,**b**) WT or *Miz1*(POZ)$^{fl/fl}$ mice were intratracheally transduced with Ad-null or Ad-Cre for 30 d. The lung tissues were isolated and expression of Miz1 and Miz1(ΔPOZ) (mRNA and protein) was analyzed by RT-PCR (**a**) or immunoblotting using a polyclonal antibody against the Miz1 C-terminus (**b**). Arrows plus numbers (3-6) in **a** indicate positions of primers. (**c**,**d**) Semi-quantitative (**c**) and qRT-PCR (**d**) analysis of the Miz1 POZ domain in ATII and hematopoietic-derived cells of the lungs of Ad-null, Ad-Cre, or Ad-SPC-Cre-infected *Miz1*(POZ)$^{fl/fl}$ mice. (**e**,**f**) BAL fluid total cell counts (**e**) and protein concentration (**f**) of WT or *Miz1*(POZ)$^{fl/fl}$ mice that were intratracheally transduced with Ad-null or Ad-Cre for 30 d and then treated with intratracheal LPS for 2 d. (**g-j**) *Miz1*(POZ)$^{fl/fl}$ mice were intratracheally transduced with Ad-null or Ad-Cre for 30 d. Lung permeability was analyzed by Evan's blue dye (EBD) extravasation into airways (**g**,**h**). Photographs of EBD extravasation from representative lungs (**g**). Quantitative analysis of EBD extravasation from lung homogenates (**h**). Alveolar-capillary permeability to a 4-kDa FITC-labeled dextran (**i**) as well as lung wet-to-dry ratio was measured (**j**). (**k**) Survival of Ad-null or Ad-Cre-treated *Miz1*(POZ)$^{fl/fl}$ mice after challenge with LPS (6 mg/kg). (**l-n**) Bone marrow cells isolated from *Miz1*(POZ)$^{fl/fl}$ mice (CD45.2$^+$) were transduced with null or Cre lentivirus and then transferred to lethally irradiated WT recipient mice (CD45.1$^+$). Expression of CD45.1 and CD45.2 in the blood cells of the chimeras was determined by flow cytometry (**l**). Expression of the Miz1 POZ domain in lung ATII and hematopoietic-derived cells of the chimeras was determined by qRT-PCR (**m**) and lung histology from PBS or LPS-treated chimeras was analyzed (**n**). Five mice per group except in **k**, in which ten mice per group, were examined (**a-n**), and data are shown as the means ± s.e.m. (**d**,**e**,**f**,**h-j**,**m**). *, P < 0.05; **, P < 0.01 by Student's *t*-test.

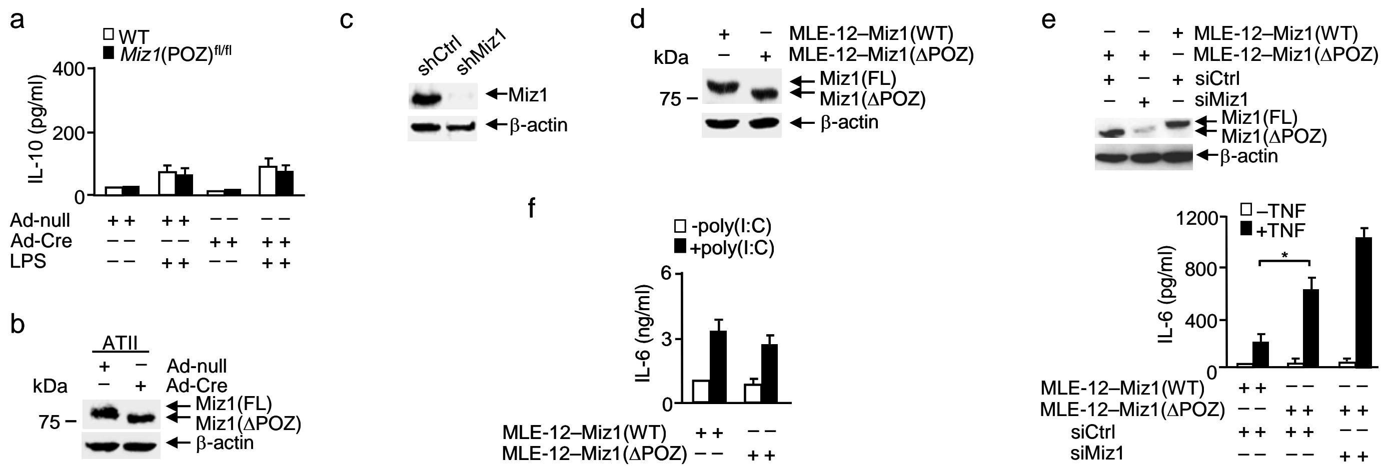

Supplementary Figure 2 The effects of loss of the Miz1 POZ domain on LPS-induced production of cytokines and inflammation in hematopoietic-derived cells of the lung. (**a**) Analysis of IL-10 production in the BAL fluid of WT or *Miz1*(POZ)$^{fl/fl}$ mice (n = 5 mice per group) that were intratracheally transduced with Ad-null or Ad-Cre for 30 d and then treated with intratracheal LPS for 8 h. (**b-d**) Immunoblotting analysis of Miz1 in ATII cells that were isolated from *Miz1*(POZ)$^{fl/fl}$ mice and infected with Ad-null or Ad-Cre (**b**), expression of Miz1 protein in MLE-12 cells stably expressing the scrambled shRNA control or shMiz1 [MLE–12/Miz1(KD)] (**c**), and Miz1 in stable MLE-12–Miz1(WT) and MLE-12–Miz1(ΔPOZ) cells (**d**). (**e**) Analysis of Miz1 expression and IL-6 production in MLE-12–Miz1(ΔPOZ) cells that were transfected with control siRNA or Miz1 siRNA and then treated with TNF. MLE-12–Miz1(WT) cells were used as control. (**f**) Poly(I:C)-induced IL-6 production in MLE-12–Miz1(WT) and MLE-12–Miz1(ΔPOZ) cells. Data are representative of three independent experiments (**a-f**) and are shown as the (means ± s.e.m.) (**a,e,f**). *, $P < 0.05$ by Student's *t*-test.

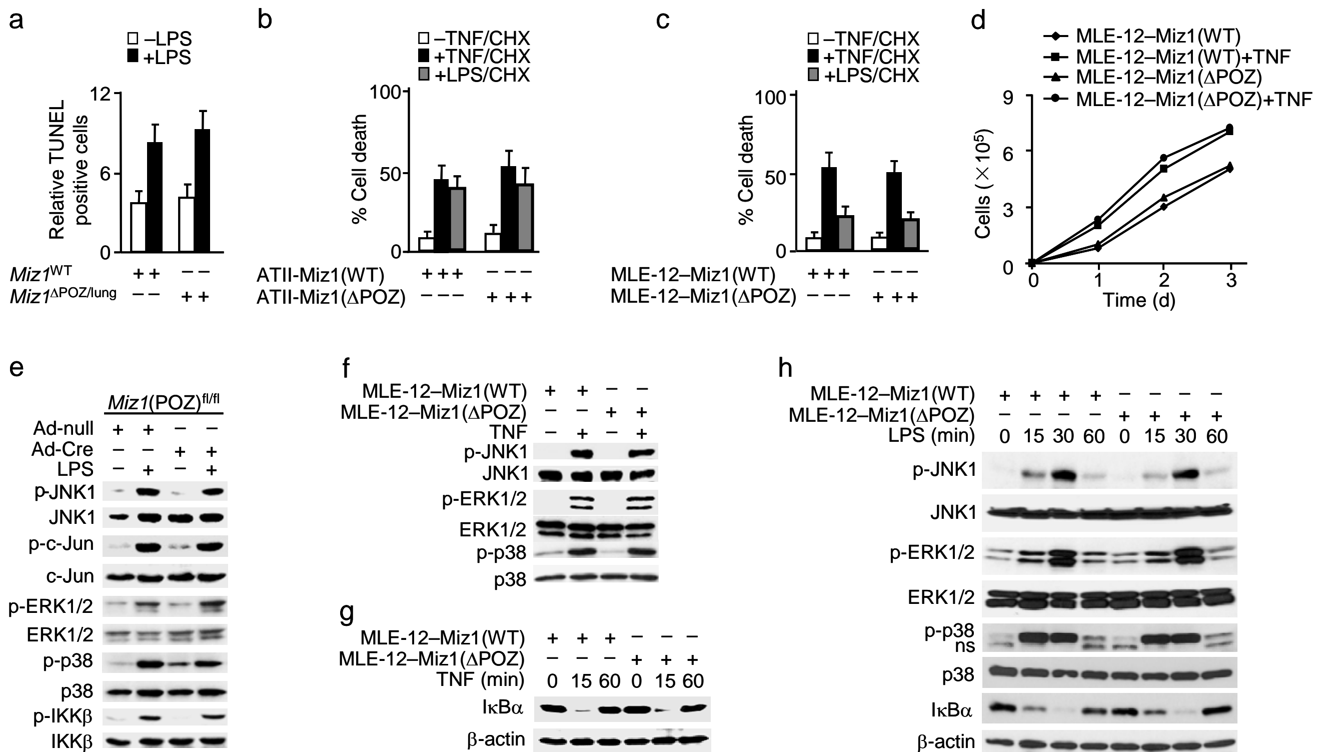

Supplementary Figure 3 Loss of the *Miz1* POZ domain does not affect lung epithelial cell death or proliferation, or activation of MAP kinases or NF-κB. (**a**) TUNEL analysis in the lungs of *Miz1*(POZ)$^{fl/fl}$ mice (n = 5 mice per group) that were intratracheally transduced with Ad-null or Ad-Cre for 30 d and then treated with intratracheal LPS for 2 d. (**b,c**) Apoptotic cell death was determined in ATII cells that were isolated from *Miz1*(POZ)$^{fl/fl}$ mice and then infected with Ad-null or Ad-Cre (**b**), or in MLE-12–Miz1(WT) and MLE-12–Miz1(ΔPOZ) cells (**c**) treated with TNF or LPS in the presence of cycloheximide (CHX). Data are representative of three independent experiments (means ± s.e.m.) (**a-c**). (**d**) Proliferation rate of MLE-12–Miz1(WT) and MLE-12–Miz1(ΔPOZ) cells that were treated without or with TNF. Data are representative of three independent experiments (average). (**e**) *Miz1*(POZ)$^{fl/fl}$ mice were intratracheally transduced with Ad-null or Ad-Cre for 30 d and then treated with or without intratracheal LPS. Activation of MAP kinases (JNK, p38, and ERK) or IKK in the lungs was determined. (**f-h**) Activation of MAP kinases (**f,h**) as well as IκBα degradation and resynthesis (**g,h**) in MLE-12–Miz1(WT) and MLE-12–Miz1(ΔPOZ) cells that were treated with or without TNF (**f,g**) or LPS (**h**). ns, non-specific. Results are representative of three independent experiments (**e-h**).

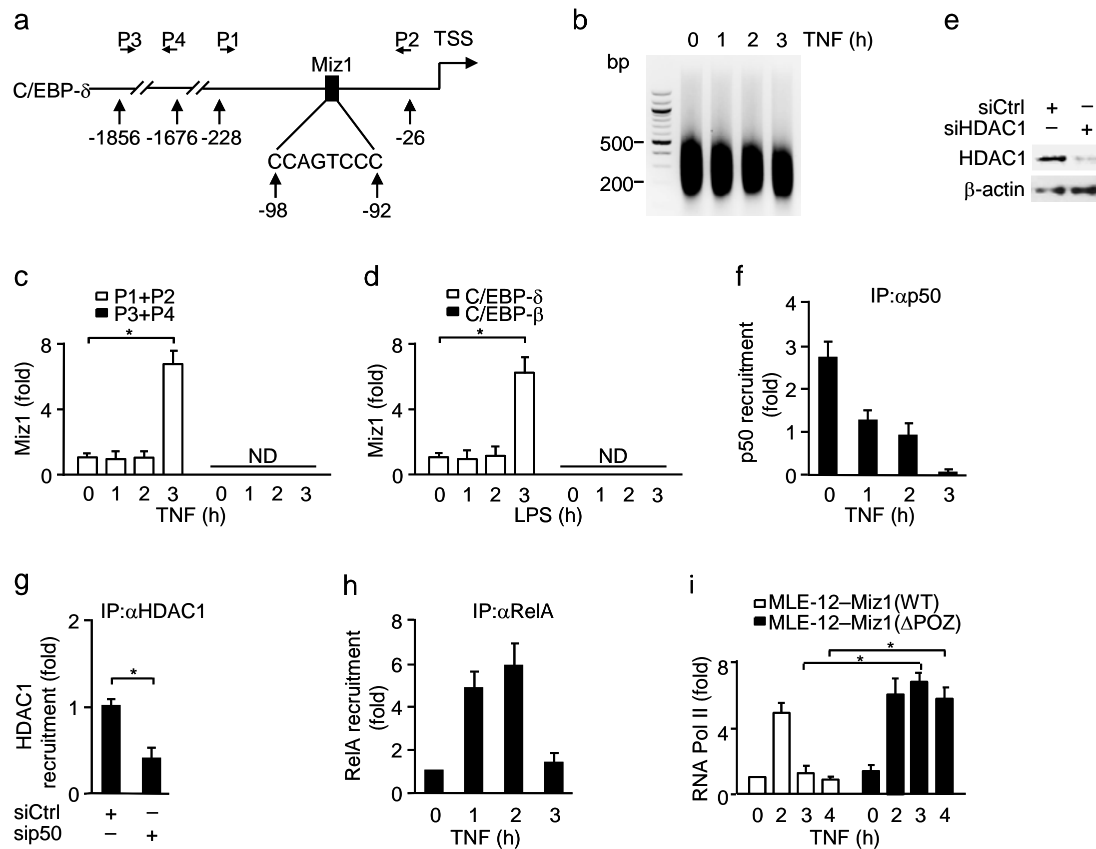

Supplementary Figure 4 Analysis of the recruitment of Miz1, p50, RelA, and HDAC1 to the *Cebpd* promoter under non-stimulated or stimulated (TNF or LPS) conditions. (**a**) Schematic presentation of the *Cebpd* promoter. TSS: transcription start site; ▌ indicates the putative Miz1 binding site; horizontal arrows with P# (P1-P4) indicate primers used for the ChIP in **c**; vertical arrows with numbers indicate positions on the promoter. (**b**) The size of chromatin after shearing in **c**. (**c**) ChIP analysis of TNF-induced Miz1 recruitment to the *Cebpd* promoter in MLE-12 cells using primers P1+P2 or P3+P4 for qPCR as indicated. (**d**) ChIP analysis of LPS-induced Miz1 recruitment to the *Cebpd* or *Cebpb* promoter in MLE-12 cells. (**e**) Immunoblotting analysis of HDAC1 in MLE-12 cells transfected with control siRNA or HDAC1 siRNA. (**f**) ChIP analysis of p50 binding on the *Cebpd* promoter in TNF-treated MLE-12 cells. (**g**) ChIP analysis of HDAC1 on the *Cebpd* promoter in MLE-12 cells transfected with control siRNA or p50 siRNA under nonstimulated conditions. (**h**) ChIP analysis of RelA on the *Cebpd* promoter in TNF-treated MLE-12 cells. (**i**) TNF-induced recruitment of RNA Polymerase II to the *Cebpd* promoter in MLE-12–Miz1(WT) and MLE-12–Miz1(ΔPOZ) cells. Data are representative of three independent experiments (**b-i**) and shown as the means ± s.e.m. (**c,d,f-i**). ND, not detected. *, $P < 0.05$ by Student's *t*-test.

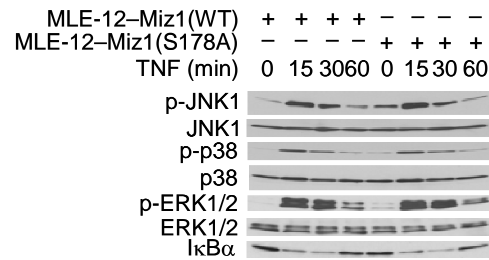

Supplementary Figure 5 Miz1 Ser178 phosphorylation is not involved in its cytoplasmic activity. MLE-12–Miz1(WT) and MLE-12–Miz1(S178A) cells were treated with or without TNF for various times as indicated. Activation of MAP kinases (JNK, p38, ERK) and IKK was determined.